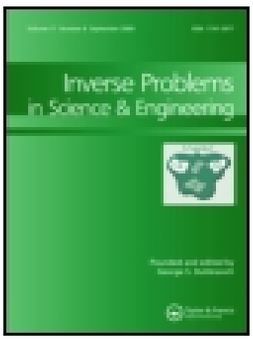

Inverse Problems in Science and Engineering

ISSN: 1741-5977 (Print) 1741-5985 (Online) Journal homepage: http://www.tandfonline.com/loi/gipe20

Finite element model updating using Hamiltonian Monte Carlo techniques

I. Boulkaibet, L. Mthembu, T. Marwala, M. I. Friswell & S. Adhikari

To cite this article: I. Boulkaibet, L. Mthembu, T. Marwala, M. I. Friswell & S. Adhikari (2016): Finite element model updating using Hamiltonian Monte Carlo techniques, Inverse Problems in Science and Engineering, DOI: 10.1080/17415977.2016.1215446

To link to this article: http://dx.doi.org/10.1080/17415977.2016.1215446

INVERSE PROBLEMS IN SCIENCE AND ENGINEERING, 2016
http://dx.doi.org/10.1080/17415977.2016.1215446

Taylor & Francis
Taylor & Francis Group

Finite element model updating using Hamiltonian Monte Carlo techniques

I. Boulkaibet[a], L. Mthembu[a], T. Marwala[a], M. I. Friswell[b] and S. Adhikari[b]

[a]The Centre for Intelligent System Modelling (CISM), Electrical and Electronic Engineering Department, University of Johannesburg, Auckland Park, South Africa; [b]College of Engineering, Swansea University Bay Campus, Swansea, UK

ABSTRACT

Bayesian techniques have been widely used in finite element model (FEM) updating. The attraction of these techniques is their ability to quantify and characterize the uncertainties associated with dynamic systems. In order to update an FEM, the Bayesian formulation requires the evaluation of the posterior distribution function. For large systems, this function is difficult to solve analytically. In such cases, the use of sampling techniques often provides a good approximation of this posterior distribution function. The hybrid Monte Carlo (HMC) method is a classic sampling method used to approximate high-dimensional complex problems. However, the acceptance rate of HMC is sensitive to the system size, as well as to the time step used to evaluate the molecular dynamics trajectory. The shadow HMC technique (SHMC), which is a modified version of the HMC method, was developed to improve sampling for large system sizes by drawing from a modified shadow Hamiltonian function. However, the SHMC algorithm performance is limited by the use of a non-separable modified Hamiltonian function. Moreover, two additional parameters are required for the sampling procedure, which could be computationally expensive. To overcome these weaknesses, the separable shadow HMC (S2HMC) method has been introduced. This method uses a transformation to a different parameter space to generate samples. In this paper, we analyse the application and performance of these algorithms, including the parameters used in each algorithm, their limitations and the effects on model updating. The accuracy and the efficiency of the algorithms are demonstrated by updating the finite element models of two real mechanical structures. It is observed that the S2HMC algorithm has a number of advantages over the other algorithms; for example, the S2HMC algorithm is able to efficiently sample at larger time steps while using fewer parameters than the other algorithms.

ARTICLE HISTORY
Received 5 April 2015
Accepted 18 July 2016

KEYWORDS
Bayesian; sampling; finite element model updating; Markov Chain Monte Carlo; molecular dynamics; Hamiltonian function; hybrid Monte Carlo method; shadow hybrid Monte Carlo; separable shadow hybrid Monte Carlo

CONTACT I. Boulkaibet boulkaibet.lyes@gmail.com

1. Introduction

The finite element model (FEM) is a method used to construct mathematical models of structures.[1,2] Due to the uncertainties and approximations associated with the process of constructing finite element models of structures, the analytical results are different from those obtained from experimental measurements.[3,4] Thus, for practical purposes, the FE model has to be updated. In recent years, the use of the Bayesian framework has shown promising results when applied to system identification problems.[4–8] This approach allows the uncertainties of the modelled systems/structures to be expressed in terms of probability, by representing the unknown parameters as random vectors with a joint probability density function (PDF). This distribution function is known as the posterior PDF. In general, the posterior PDF is not analytically available for sufficiently complex problems. This is the case for the FEM updating problem, where the parameter search space is non-linear and high dimensional.

To cope with this problem, Beck and Katafygiotis [9] employed Laplace's method of asymptotic approximation to estimate the uncertain parameters. In this method, a Gaussian approximation is used to predict the posterior PDF. This approach can be computationally challenging because of the complications caused by the non-convex optimization required. This method is only valid if a large amount of data is available, and convergence may not occur if the chosen initial values are too far from the neighbourhood of the high probability region.

In problems where the uncertain parameter search space is large and complex, sampling techniques can be more useful. Different methods such as multivariate normal sampling (MNS),[10] Latin hypercube sampling (LHS) [11] and orthogonal array sampling [12] have been employed to find the most probable values of the uncertain parameters. MNS techniques can only be applied for uncertain parameters that have a Gaussian PDF. This method is easily implemented when the uncertain parameters are uncorrelated and the covariance matrix is a diagonal matrix. However, difficulties may arise when the uncertain parameters are correlated, and the accuracy of this method will rapidly decrease. The LHS technique was introduced by McKay et al. [11]. In this method, the parameter space is divided into subspaces of equal probability and samples are taken from each subspace equally. This method is very effective when only one parameter is sampled but becomes more complex and computationally expensive when high-dimensional problems are targeted since the method has to cover all possible combinations. Haddad Khodaparast [10] applied both the Multivariate Normal Sampling and Latin Hypercube Sampling methods to model updating. The orthogonal array (OA) sampling [12] method represents a modified version of the LHS methods. However, OA sampling produces uniform samples in multiple dimensions while the LHS method produces a uniform sampling in one dimension only (LHS is a special case of an OA sampler). Unfortunately, the results obtained from the previous three sampling algorithms (MNS, LHS and OA) are highly sensitive to the complexity of the system and the size of the search space.

In contrast, Markov Chain Monte Carlo (MCMC) methods are established sampling methods that can offer a very practical solution to estimate the desired posterior distribution function in a reasonable time.[4,7,13,14] The Metropolis–Hastings (M–H) algorithm is the most popular MCMC algorithm [15,16] and has been applied in various scientific fields. This algorithm generates samples from a target distribution by applying an acceptance–rejection

criterion to accept new samples, while a proposed PDF is used to suggest the new sample candidate. Geometrically, the proposed PDF constructs a random walk trajectory during the search. Unfortunately, the algorithm's performance becomes poor when the modelled system is complicated since the M–H acceptance rate decreases causing a mixing of the sampling chain. The M–H algorithm has been employed many times in model updating, see [4,7] for more information. Based on the M–H algorithm, Beck and Au [17] proposed an adaptive Metropolis–Hastings (AMH) method where instead of drawing samples from the target PDF, the samples are obtained from a series of simpler intermediate probability density functions (PDFs) that converge to the target PDF. The AMH algorithm was found to be useful for problems with flat, very peaked and multimodal target PDFs. However, this approach is inefficient for high-dimensional problems since kernel density estimation is required for this approach. Another popular MCMC algorithm called the 'Gibbs sampler' [18] has been used to update structures. This algorithm can be used to generate samples from undefined PDFs (see [19]). Ching and Cheng [20] proposed the Transitional Markov Chain Monte Carlo (TMCMC) algorithm which is based on the adaptive M–H algorithm. This algorithm is more efficient than the AMH method. The TMCMC algorithm can avoid the complexities of sampling from a difficult target using a series of intermediate PDFs that converge to the target PDF. Moreover, the TMCMC approach has the ability to automatically select the intermediate PDFs. The use of the TMCMC algorithm has greatly increased in model updating since Muto and Beck [21] applied it to update hysteretic structural models. Also, the TMCMC algorithm can be used as a parallel algorithm for more complex problems. Unfortunately, the TMCMC algorithm is fundamentally based on the general M–H algorithm where the random walk trajectory is restricted in complex systems. The performance of these algorithms decreases with the complexity as well as the size of the modelled system.

Another class of MCMC algorithms, the Hybrid Monte Carlo algorithm, also known as the Hamiltonian Monte Carlo (HMS) method, was first introduced in the physics literature by Duane et al. [22]. The HMC method has a Molecular Dynamic move trajectory that has the ability to deal with large and complicated systems. The HMC method locates high probability search regions quicker and with fewer iterations which is not the case with algorithms that have random walk trajectories. The HMC trajectory is guided by the derivative of the target log-density probability (the log-posterior derivative).[7,13,23,24] The core step of this algorithm is to introduce an auxiliary variable/vector, called the momentum vector, to create a new molecular dynamic (MD) system while the uncertain parameter vector is treated as the system displacement. The total energy of the new MD system, which is called the Hamiltonian function, contains both a potential energy, which is equal to the log-posterior, and a kinetic energy based on the momentum vector. The velocity Verlet (VV), also called the leapfrog algorithm, is used to evaluate the total energy of this MD system. The HMC method was first proposed in model updating by Cheung and Beck [25], who successfully updated a linear structural dynamic model with 31 parameters. The Bayesian method based on the HMC sampling algorithm successfully characterized the modelling uncertainties associated with the underlying structural system (see [25] for more details).

However, the VV integrator does not conserve energy, especially when the time step used and/or the system size is considered to be large. To overcome these limitations, a modified HMC algorithm based on a modified Hamiltonian function, called the Shadow Hybrid Monte Carlo (SHMC), was proposed in [26]. The SHMC is based on the HMC method but it uses an approximation of the modified Hamiltonian, also called a Shadow

Hamiltonian function, to sample through the phase space in an efficient way. Boulkaibet et al. [27] implemented the SHMC to update an unsymmetrical H-shaped structure and the GARTEUR SM-AG19 structure. The SHMC technique and the HMC algorithm give good updated results. However, the results obtained by the SHMC algorithm for a relatively large time step are more accurate than the HMC results; when the time step increases, the sampling rate of the HMC decreases which leads to poor algorithm performance. However, the SHMC uses a non-separable Hamiltonian function that generates the moments in a computationally expensive way. The SHMC method also requires extra parameters to stabilize the rejection cost for both moments and positions while an augmented VV Integrator is used to evaluate the shadow Hamiltonian function.[26,27]

In this paper, the separable shadow hybrid Monte Carlo (S2HMC) [28,29] is adopted to update real structural systems. The S2HMC samples from the posterior PDF using a separable shadow Hamiltonian function and without involving any extra parameters. In this paper, the efficiency, reliability and limitations of the S2HMC technique are investigated when a Bayesian approach is applied to an FEM updating problem. The results obtained are compared with those obtained by the SHMC algorithm in [27]. In the next section, Bayesian inference is introduced and the posterior distribution of the uncertain parameters of the FEM is presented. Section 3 presents the Hamiltonian dynamics and describes the basic HMC algorithm. Section 4 introduces the Separable Shadow Hamiltonian method. Section 5 presents the implementation of some of these algorithms on the unsymmetrical H-shaped beam structure. Section 6 presents the implementation of these algorithms on the GARTEUR SM-AG19 structure. Finally, Section 7 concludes the paper.

2. Bayesian inference

In order to update a mathematical model, the uncertain parameters of the model have to be identified and quantified. Bayes' theorem offers the ability to quantify the uncertainty associated with the model parameters.[4,5] In this paper, Bayesian theory is used to identify the uncertain parameters in the FEM updating problem. Bayesian approaches are governed by Bayes' rule [4,5,7,27,30]:

$$P\left(\boldsymbol{\theta}|\mathcal{D},\boldsymbol{\mathcal{M}}\right) \propto P\left(\mathcal{D}|\boldsymbol{\theta},\boldsymbol{\mathcal{M}}\right)P(\boldsymbol{\theta}|\boldsymbol{\mathcal{M}}) \tag{1}$$

$\boldsymbol{\mathcal{M}}$ represents the probabilistic model class for the target system. The model class is defined by the parameters of the model, $\boldsymbol{\theta} \in \boldsymbol{\Theta} \subset \mathcal{R}^D$, where a different set of the vector $\boldsymbol{\theta}$ represents a different class $\boldsymbol{\mathcal{M}}$. $\mathcal{D}$ represents the modal properties obtained from experiments (natural frequencies, f_i^m, and mode shapes, $\boldsymbol{\phi}_i^m$). The quantity $P(\boldsymbol{\theta}|\boldsymbol{\mathcal{M}})$ is the prior probability density function (PDF) of the updating parameters, given the assumed model class $\boldsymbol{\mathcal{M}}$ in the absence of the data $\mathcal{D}$. The quantity $P(\boldsymbol{\theta}|\mathcal{D},\boldsymbol{\mathcal{M}})$ describes the posterior PDF of the parameters in the presence of the data $\mathcal{D}$ and the assumed model class $\boldsymbol{\mathcal{M}}$. $P(\mathcal{D}|\boldsymbol{\theta},\boldsymbol{\mathcal{M}})$ is the likelihood function, which represents the probability of the data ($\mathcal{D}$) in the presence of the uncertain parameters $\boldsymbol{\theta}$ and the assumed model class $\boldsymbol{\mathcal{M}}$.[4,7,27] The dependence on the model class $\boldsymbol{\mathcal{M}}$ is only important when more than one model class is investigated and a class selection is needed to identify the better class of model. In this work, only one model class is investigated and hence the dependence on the model class $\boldsymbol{\mathcal{M}}$ is omitted to simplify the notation.

The likelihood function is given by [4,7,27]

$$P(\mathcal{D}|\boldsymbol{\theta}) = \frac{1}{\left(\frac{2\pi}{\beta_c}\right)^{N_m/2}\prod_{i=1}^{N_m} f_i^m}\exp\left(-\frac{\beta_c}{2}\sum_i^{N_m}\left(\frac{f_i^m - f_i^a}{f_i^m}\right)^2\right) \tag{2}$$

where β_c is a constant and can be used to weight the likelihood terms in the posterior, N_m is the number of measured modes f_i^m and f_i^a is the ith analytical natural frequency obtained from the finite element model. In this paper, only natural frequencies are considered.

The prior PDF represents the prior knowledge of the updating parameters $\boldsymbol{\theta}$.[8] Here, this PDF is assumed to be Gaussian [4,7,27]

$$\begin{aligned} P(\boldsymbol{\theta}) &= \frac{1}{(2\pi)^{Q/2}\prod_{j=1}^{Q}\frac{1}{\sqrt{\alpha_j}}}\exp\left(-\sum_j^Q\frac{\alpha_j}{2}\left\|\boldsymbol{\theta}^j - \boldsymbol{\theta}_0^j\right\|^2\right) \\ &= \frac{1}{(2\pi)^{Q/2}\prod_{j=1}^{Q}\frac{1}{\sqrt{\alpha_j}}}\exp\left(-\frac{1}{2}(\boldsymbol{\theta}-\boldsymbol{\theta}_0)^T\Sigma^{-1}(\boldsymbol{\theta}-\boldsymbol{\theta}_0)\right) \end{aligned} \tag{3}$$

where $\boldsymbol{\theta}_0$ represents the mean value of the uncertain parameters, Q is the number of uncertain parameters to be identified and α_j is the coefficient of the prior PDF for the jth updating parameter (which is related to the variance by $\alpha_j = \frac{1}{\sigma_j^2}$). The notation $\| * \|$ denotes the Euclidean norm of the term *.

The posterior PDF of the parameters $\boldsymbol{\theta}$, given the observed data $\mathcal{D}$, is derived by applying Bayes' theorem from Equation (1). The density function $P(\boldsymbol{\theta}|\mathcal{D})$ is calculated by substituting Equations (2) and (3) into Equation (1) to give

$$P(\boldsymbol{\theta}|\mathcal{D}) \propto \frac{1}{Z_s(\alpha,\beta_c)}\exp\left(-\frac{\beta_c}{2}\sum_i^{N_m}\left(\frac{f_i^m - f_i^a}{f_i^m}\right)^2 - \sum_j^Q\frac{\alpha_j}{2}\left\|\boldsymbol{\theta}^j - \boldsymbol{\theta}_0^j\right\|^2\right) \tag{4}$$

where

$$Z_s(\alpha,\beta_c) = \left(\frac{2\pi}{\beta_c}\right)^{N_m/2}\prod_{i=1}^{N_m} f_i^m (2\pi)^{Q/2}\prod_{j=1}^{Q}\frac{1}{\sqrt{\alpha_j}} \tag{5}$$

In most cases, obtaining the analytical form of the posterior PDF is not possible. In these cases, sampling methods are used to provide an approximate solution. Sampling techniques can simplify Bayesian inference by providing a set of random samples from the posterior distribution.[4,7,27] If Y is an observation of certain parameters at different discrete time instants, then the prediction of the future responses of this parameter Y at different time instants could be achieved by the total probability theorem as

$$P(Y|D) = \int_{\boldsymbol{\theta}} P(Y|\boldsymbol{\theta})P(\boldsymbol{\theta}|D)\mathrm{d}\boldsymbol{\theta} \tag{6}$$

Equation (6) depends on the posterior PDF and sampling techniques such as the Markov Chain Monte Carlo (MCMC) methods can be easily employed to estimate the unknown parameters. Given a set of N_s random parameter vectors drawn from $P(\boldsymbol{\theta}|D)$, the expectation

value of any observed function Y can be estimated by approximating the integral in Equation (6) by

$$\tilde{Y} \cong \frac{1}{N_s} \sum_{i=1}^{N_s} G(\boldsymbol{\theta}_i) \tag{7}$$

where G is a function that depends on the unknown parameters $\boldsymbol{\theta}_i$. In this paper, the S2HMC, SHMC and HMC methods are used to sample from the posterior PDF and the results are compared.

3. Hamiltonian dynamics

In an HMC algorithm, a dynamic system is considered in which auxiliary variables called momentum, $\mathbf{p} \in R^N$, are introduced. The updated vector $\boldsymbol{\theta}$ is treated as a displacement. The total energy, also known as the Hamiltonian function, of the new dynamic system is defined by $H(\boldsymbol{\theta}, \mathbf{p}) = V(\boldsymbol{\theta}) + W(\mathbf{p})$, where the potential energy is defined by $V(\boldsymbol{\theta}) = -\ln(P(\boldsymbol{\theta}|D))$ and the kinetic energy $W(\mathbf{p}) = \mathbf{p}^{\mathbf{T}}\mathbf{M}^{-1}\mathbf{p}/2$, which depends only on $\mathbf{p}$ and some chosen positive definite matrix $\mathbf{M} \in R^{N\times N}$. The Hamiltonian method is a half-stochastic, hybrid approach that has a Molecular Dynamic trajectory. This property can be very useful when the HMC algorithm is implemented for large and complicated systems.[6,7,23,27,31] This method is hybrid because it combines a molecular dynamic (MD) trajectory with a Monte Carlo (MC) acceptance–rejection step.[23]

The Hamiltonian dynamic system associated with $H(\boldsymbol{\theta}, \mathbf{p})$ is governed by the following equations:

$$\frac{\mathrm{d}\boldsymbol{\theta}}{\mathrm{d}t} = \mathbf{M}^{-1}\mathbf{p}(t), \qquad \frac{\mathrm{d}\boldsymbol{p}}{\mathrm{d}t} = -\nabla V(\boldsymbol{\theta}(t)) \tag{8}$$

The Hamiltonian function can be used to define a joint distribution, which can be written as $f(\boldsymbol{\theta}, \mathbf{p}) \propto \exp(-\beta_B H(\boldsymbol{\theta}, \mathbf{p}))$where $\beta_B = \frac{1}{K_B T}$and K_B is a Boltzmann constant and T is temperature. In this paper, the Hamiltonian dynamic system PDF function $f(\boldsymbol{\theta}, \mathbf{p})$ is considered to follow a Boltzmann distribution. The canonical ensemble (also known as 'NVT' for constant temperature T, constant volume V and constant number of particles N), is used to perform the Molecular Dynamic simulation. A nice feature of this ensemble is that position $\boldsymbol{\theta}$ and momentum $\mathbf{p}$ are independent for separable Hamiltonians.[32]

The evolution of $(\boldsymbol{\theta}, \mathbf{p})$ through time t can be achieved numerically using the VV (leapfrog) scheme [7,8]

$$\mathbf{p}\left(t + \frac{\delta t}{2}\right) = \mathbf{p}(t) - \frac{\delta t}{2}\nabla V(\boldsymbol{\theta}(t)) \tag{9}$$

$$\boldsymbol{\theta}(t + \delta t) = \boldsymbol{\theta}(t) + \delta t \mathbf{M}^{-1}\mathbf{p}\left(t + \frac{\delta t}{2}\right) \tag{10}$$

$$\mathbf{p}(t + \delta t) = \mathbf{p}\left(t + \frac{\delta t}{2}\right) - \frac{\delta t}{2}\nabla V(\boldsymbol{\theta}(t + \delta t)) \tag{11}$$

where δt is the time step and ∇V is obtained numerically by finite differences as

$$\frac{\partial V}{\partial \theta_i} = \frac{V(\boldsymbol{\theta} + \Delta h) - V(\boldsymbol{\theta} - \Delta h)}{2h\Delta_i} \tag{12}$$

$\Delta = \left[\Delta_1, \Delta_2, \ldots, \Delta_N\right]^T$ is the perturbation vector and h is a scalar that dictates the size of the perturbation of $\boldsymbol{\theta}$.

After each iteration of Equations (9)–(11), the resulting candidate state is accepted or rejected according to the Metropolis criterion based on the value of the Hamiltonian $H(\boldsymbol{\theta}, \mathbf{p})$. The HMC algorithm can be summarized as follows:

(1) Use $\boldsymbol{\theta}_0$ to initiate the algorithm.
(2) Initiate $\mathbf{p}_0$ such that $\mathbf{p}_0 \sim N(0, \boldsymbol{M})$.
(3) The leapfrog algorithm is initiated with $(\boldsymbol{\theta}, \mathbf{p})$ and the algorithm is evaluated for L time steps to obtain $(\boldsymbol{\theta}^*, \mathbf{p}^*)$.
(4) Use $\boldsymbol{\theta}^*$ to update the FEM and to obtain the new analytic frequencies f_i^a and then compute $H(\boldsymbol{\theta}^*, \mathbf{p}^*)$.
(5) Accept $(\boldsymbol{\theta}^*, \mathbf{p}^*)$ with probability $\min\left(1, \exp\left\{-\beta_B \Delta H\right\}\right)$.

Repeat steps (3)–(5) for N_s samples.

Here, $\Delta H = H(\boldsymbol{\theta}^*, \mathbf{p}^*) - H(\boldsymbol{\theta}, \mathbf{p})$, and the estimated mean value of the uncertain parameters is

$$\hat{\boldsymbol{\theta}} = E(\boldsymbol{\theta}) \cong \frac{1}{N_s} \sum_{i=1}^{N_s} \boldsymbol{\theta}^{\boldsymbol{i}} \tag{13}$$

where the $E(*)$ describes the mean value of a quantity *. The variance of the uncertain parameters is

$$V\left(\hat{\boldsymbol{\theta}}\right) = E\left(\left(\boldsymbol{\theta} - \hat{\boldsymbol{\theta}}\right)^2\right) \cong \frac{1}{N_s} \sum_{i=1}^{N_s} \left(\boldsymbol{\theta}^{\boldsymbol{i}} - \hat{\boldsymbol{\theta}}\right)^2 \tag{14}$$

where the standard deviation (the errors) is given by $\boldsymbol{\sigma}_{\boldsymbol{\theta}} = \sqrt{V\left(\hat{\boldsymbol{\theta}}\right)}$.

The distance vector $\boldsymbol{\mathcal{L}}$ represents the move of the pair $(\boldsymbol{\theta}, \mathbf{p})$ in the search space after one evolution, where this vector depends on the time step δt. In this case, a relatively large time step δt is needed to ensure a significant move from the existing sample to a new one. This allows for fast convergence and better exploration of the search space. Unfortunately, due to the numerical errors caused by the Verlet integrator, the performance of the HMC method degrades when the time step is large. This may be due to the fluctuation of the Hamiltonian function which then causes an increase in the rejection rate of the algorithm. This means no samples are accepted when $\delta t \geq \delta t_{\max}$, where $\delta t_{\max}$ represents the upper bound of the time step. In such cases, the time step of the HMC algorithm should be less than $\delta t_{\max}$ to avoid a large rejection rate. On the other hand, a too small δt stabilizes the Hamiltonian function and gives a high acceptance rate of the HMC algorithm. However, a large number of samples will be needed to cover more space during the search (especially when $\delta t \leq \delta t_{\min}$, where $\delta t_{\min}$ represents the lower bound of the time step).

Cheung et al. [6] maximized the distance $\mathcal{L}(\delta t)$ using a small number of samples and empirically explored different δt to achieve the maximum $\mathcal{L}(\delta t)$. However, this method is not efficient, especially when the algorithms search near space boundaries. Another approach to the time step problems is to use a variable step size (adaptive time step). Huang et al. [33] proposed an adaptive Verlet method, which is based on time re-parameterization. A new variable is introduced into the leapfrog scheme and this variable τ is related to a chosen smooth scalar-valued function. However, the adaptive Verlet method still has limitations where the time step is still considered small within this method (the bounds of the time step are applied). To overcome this inconvenience, the shadow Hybrid Monte Carlo (SHMC) algorithm (with a modified Hamiltonian function) was proposed in [26]. This algorithm has the ability to produce samples with a relatively large time step. In SHMC algorithm, a modified Hamiltonian function $\tilde{H}\left(\boldsymbol{\theta}, \boldsymbol{p}\right)$ is exploited to sample from an extended phase space of the shadow Hamiltonian rather than sampling from a configuration space. [26,27] The SHMC formulation requires the introduction of a constant c in the modified Hamiltonian function $\tilde{H}\left(\boldsymbol{\theta}, \mathbf{p}\right)$, while the density function $\tilde{f}\left(\boldsymbol{\theta}, \mathbf{p}\right) \propto \exp\left(-\beta_B \tilde{H}\left(\boldsymbol{\theta}, \mathbf{p}\right)\right)$ is used to obtain samples. In the SHMC algorithm, the proposed modified Hamiltonian function is defined as $\tilde{H}\left(\boldsymbol{\theta}, \mathbf{p}\right) = \max\left(H(\boldsymbol{\theta}, \mathbf{p}), H_{[2k]}\left(\boldsymbol{\theta}, \boldsymbol{p}\right) - c\right)$. The function $H_{[2k]}\left(\boldsymbol{\theta}, \boldsymbol{p}\right)$ is a shadow Hamiltonian of an order $2k$, where the shadow Hamiltonian functions of orders 4 and 8 are described in [26,27]. The SHMC algorithm of order $2k$ is summarized as following [26,27]:

(1) Set the initial value $\boldsymbol{\theta}_0$
(2) Repeat for N_S samples:

Monte Carlo (MC) step:

(a) Produce $\boldsymbol{p}$ such that $\boldsymbol{p} \sim N(0, \boldsymbol{M})$
(b) Accept with probability

$$\min\left(1,\ \exp\left\{-\beta_B\left(H_{[2k]}\left(\boldsymbol{\theta}, \boldsymbol{p}\right) - c - H(\boldsymbol{\theta}, \mathbf{p})\right)\right\}\right)$$

(c) Repeat until a new $\boldsymbol{p}$ is accepted

Molecular Dynamic (MD) step:

(a) Initialize the extended leapfrog algorithm with $(\boldsymbol{\theta}, \mathbf{p})$ and run the algorithm for L time steps to obtain $(\boldsymbol{\theta}^*, \mathbf{p}^*)$
(b) Update the FEM to obtain the new analytical frequencies and then compute $\tilde{H}\left(\boldsymbol{\theta}^*, \boldsymbol{p}^*\right)$
(c) Accept $(\boldsymbol{\theta}^*, \mathbf{p}^*)$ with the probability $\min\left(1, \exp\left\{-\beta_B \Delta \tilde{H}\right\}\right)$

Unfortunately, the non-separable Hamiltonian function $H_{[2k]}\left(\boldsymbol{\theta}, \boldsymbol{p}\right)$ used in this algorithm causes disadvantages such as the computational expense in generating the momentum estimates.[27] Furthermore, this method requires an extra tuning parameter to balance the cost of rejection of momentum and positions.

In this paper, the S2HMC algorithm which uses a separable shadow Hamiltonian function to sample the posterior distribution function of the FEM updating parameters is investigated. This approach does not require any extra parameters. The results obtained by the

S2HMC algorithm will be compared to those obtained by the HMC and SHMC algorithms in [27].

4. The separable shadow Hamiltonian method

The separable shadow hybrid Monte Carlo (S2HMC) [28] algorithm is a modified version of the SHMC algorithm where a separable shadow Hamiltonian function is employed to generate samples. A shadow Hamiltonian function represents an accurate approximation to the Hamiltonian function which is conserved more closely than the original Hamiltonian function when a large time step is used during the evolution of the Verlet integrator. However, the use of the shadow Hamiltonian function can complicate the sampling procedure of the momentum vector. The S2HMC method improves the sampling efficiency by sampling from a *separable* shadow Hamiltonian function, which changes the configuration spaces. These transformations prevent the use of extra parameters (such as the constant c in the SHMC algorithm) and avoid the complication of using an augmented integrator. Moreover, the procedure of sampling a new momentum vector will be similar to the HMC algorithm. These improvements can accelerate the convergence of averages computed by the method. [28] The transformations used can improve the acceptance rate with a comparatively negligible computational cost.

The S2HMC algorithm employs a processed velocity Verlet (VV) integrator to increase the order of accuracy of the sampling procedure. This can be done by changing the configuration space by introducing pre-processing and post-processing steps.[28,29] The modified Hamiltonian function used in this algorithm is conserved to $O\left(\delta t^4\right)$ by the processed method, instead of just $O\left(\delta t^2\right)$ by the unprocessed method. Similar to the SHMC algorithm, the S2HMC algorithm also requires a reweighting step to compensate for the modification of the potential energy. The shadow Hamiltonian function used in the S2HMC method is separable and of fourth order [28]:

$$\tilde{H}\left(\boldsymbol{\theta},\mathbf{p}\right)=\frac{1}{2}\mathbf{p}^{\mathbf{T}}\mathbf{M}^{-1}\mathbf{p}+V(\boldsymbol{\theta})+\frac{\delta t^2}{24}V_{\boldsymbol{\theta}}^{T}\mathbf{M}^{-1}V_{\boldsymbol{\theta}}+O\left(\delta t^4\right) \tag{15}$$

where $V_{\boldsymbol{\theta}}$ is the derivative of the potential energy V with respect to $\boldsymbol{\theta}$. The joint distribution derived from the separable shadow Hamiltonian function can be written as $\tilde{f}\left(\boldsymbol{\theta},\mathbf{p}\right)\propto\exp\left(-\beta_B\tilde{H}\left(\boldsymbol{\theta},\mathbf{p}\right)\right)$. The separable shadow Hamiltonian function is derived by applying backward error analysis to the numerical integrator.[28]

The pre-processing step is

$$\hat{\mathbf{p}}=\mathbf{p}-\frac{\delta t}{24}\left(V_{\boldsymbol{\theta}}\left(\boldsymbol{\theta}+\delta t\mathbf{M}^{-1}\hat{\mathbf{p}}\right)-V_{\boldsymbol{\theta}}\left(\boldsymbol{\theta}-\delta t\mathbf{M}^{-1}\hat{\mathbf{p}}\right)\right) \tag{16}$$

$$\hat{\boldsymbol{\theta}}=\boldsymbol{\theta}+\frac{\delta t^2}{24}\mathbf{M}^{-1}\left(V_{\boldsymbol{\theta}}\left(\boldsymbol{\theta}+\delta t\mathbf{M}^{-1}\hat{\mathbf{p}}\right)+V_{\boldsymbol{\theta}}\left(\boldsymbol{\theta}-\delta t\mathbf{M}^{-1}\hat{\mathbf{p}}\right)\right) \tag{17}$$

Equations (16) and (17) require an iterative solution for $\hat{\mathbf{p}}$ and a direct computation for $\hat{\boldsymbol{\theta}}$. The post-processing step is

$$\boldsymbol{\theta}=\hat{\boldsymbol{\theta}}-\frac{\delta t^2}{24}\mathbf{M}^{-1}\left(V_{\boldsymbol{\theta}}\left(\boldsymbol{\theta}+\delta t\mathbf{M}^{-1}\hat{\mathbf{p}}\right)+V_{\boldsymbol{\theta}}\left(\boldsymbol{\theta}-\delta t\mathbf{M}^{-1}\hat{\mathbf{p}}\right)\right) \tag{18}$$

$$\mathbf{p} = \hat{\mathbf{p}} + \frac{\delta t}{24}\left(V_\theta\left(\theta + \delta t \mathbf{M}^{-1}\,\hat{\mathbf{p}}\right) - V_\theta\left(\theta - \delta t \mathbf{M}^{-1}\,\hat{\mathbf{p}}\right)\right) \tag{19}$$

Equations (18) and (19) require an iterative solution for $\boldsymbol{\theta}$ and a direct computation for $\mathbf{p}$. To calculate balanced values of the mean, the results must be reweighted. The average of an observable A is given by [28]:

$$\langle A \rangle = \frac{\sum_{i=1}^{Ns} A.a_i}{\sum_{i=1}^{Ns} a_i}, \quad \text{where} \quad a_i = \frac{\exp(-\beta_B H(\boldsymbol{\theta}, \mathbf{p}))}{\exp(-\beta_B \tilde{H}\,(\boldsymbol{\theta}, \mathbf{p}))} \tag{20}$$

The S2HMC algorithm can be summarized as follows [26]:

(1) An initial value $\boldsymbol{\theta}_0$ is used to initiate the algorithm.
(2) Initiate $\mathbf{p}_0$ such that $\mathbf{p}_0 \sim N(0, \boldsymbol{M})$.
(3) Compute the initial shadow energy $\tilde{H}\,(\boldsymbol{\theta}, \mathbf{p})$ using Equation (15).
(4) Pre-processing: Starting from $(\boldsymbol{\theta}, \mathbf{p})$, solve iteratively for $\hat{\mathbf{p}}$ and directly compute $\hat{\boldsymbol{\theta}}$ using Equations (16) and (17).
(5) Initiate the leapfrog algorithm with $\left(\hat{\boldsymbol{\theta}}, \hat{\mathbf{p}}\right)$ and run for L time steps to obtain $\left(\hat{\boldsymbol{\theta}}^*, \hat{\mathbf{p}}^*\right)$ (Equations (9)–(11)).
(6) Post-processing: Starting from $\left(\hat{\boldsymbol{\theta}}^*, \hat{\mathbf{p}}^*\right)$, solve iteratively for $\boldsymbol{\theta}^*$ and a directly compute $\mathbf{p}^*$ using Equations (18) and (19).
(7) Update the FEM to obtain the new analytic frequencies and then compute $H(\boldsymbol{\theta}^*, \mathbf{p}^*)$.
(8) Accept $(\boldsymbol{\theta}^*, \mathbf{p}^*)$ with probability $\min\left(1, \exp\left\{-\beta_B \Delta\, \hat{H}\right\}\right)$.
(9) Repeat steps (3)–(8) to get N_s samples.
(10) Compute weight: use Equation (20) to compute the averages of a quantity A($\boldsymbol{\theta}$).

The idea of the constructed processed integrator is to change the phase space (pre-processing) of the pair $(\boldsymbol{\theta}, \mathbf{p})$ so that the propagation is performed in a different space and using another integrator (which has a non-separable shadow Hamiltonian). The post-processor step is evaluated when the output is required. In this way, the momentum sampling procedure is simplified and an accurate and faster simulation is guaranteed.[34]

Small changes can be made to improve the S2HMC method. The momentum vector can be effectively sampled by avoiding the dependency between their components when the momentum is drawn. The best way to deal with the dependencies between components (which are unavoidable) is to use an ordered over-relaxation approach to suppress the random walk that can happen in the momentum sampling process.[35]

The finite difference approximations defined in Equation (12) are employed to compute the gradient V_θ. This gradient is based on forward and backward Taylor series expansions of the function and is more accurate than the forward/backward difference approximation. However, when the dimension of the uncertain parameters is high, forward difference approximation could be more practical since it requires d (d is the dimension of the uncertain parameters) evaluations of $V(\boldsymbol{\theta})$ to compute the gradient, while the central difference approximation requires $2d$. The new gradient is given by $\frac{\partial V}{\partial \theta_i} = \frac{V(\boldsymbol{\theta}+\Delta h)-V(\boldsymbol{\theta})}{2h\Delta_i}$. When significant data are required to compute the gradient, it becomes computationally expensive. Instead, a subset of the data can be used to compute a noisy gradient, called a stochastic gradient. [36,37]

Table 1. The Momentum, MD and reweighting steps for HMC, SHMC and S2HMC algorithms.

Methods	Sampling new momentums (MC) step	The MD step	Reweighting step
HMC	Given $\boldsymbol{\theta}$, generate $\boldsymbol{p}$ such that $\mathbf{p} \sim N(0, \boldsymbol{M})$	Accept $(\boldsymbol{\theta}^*, \mathbf{p}^*)$ with probability $\min\left(1, \exp\left\{-\beta_B \Delta H\right\}\right)$.	
SHMC	Given $\boldsymbol{\theta}$, generate $\boldsymbol{p}$ such that $\boldsymbol{p} \sim N(0, \boldsymbol{M})$ Accept with probability: $\min\left(1, \exp\left\{-\beta_B\left(H_{[2k]}(\boldsymbol{\theta}, \boldsymbol{p}) - c - H(\boldsymbol{\theta}, \mathbf{p})\right)\right\}\right)$,	Accept $(\boldsymbol{\theta}^*, \mathbf{p}^*)$ with probability $\min\left(1, \exp\left\{-\beta_B \Delta \tilde{H}\right\}\right)$. $\tilde{H} = \max(H(\boldsymbol{\theta}, \boldsymbol{p}), H_{[2k]}(\boldsymbol{\theta}, \boldsymbol{p}) - c)$	The observable B is given by: $\langle B \rangle = \frac{\sum_{i=1}^{Ns} B.a_i}{\sum_{i=1}^{Ns} a_i}$, where $a_i = \frac{\exp(-\beta_B H(\boldsymbol{\theta}, \mathbf{p}))}{\exp(-\beta_B \tilde{H}(\boldsymbol{\theta}, \mathbf{p}))}$
S2HMC	Given $\boldsymbol{\theta}$, generate $\boldsymbol{p}$ such that $\mathbf{p} \sim N(0, \boldsymbol{M})$ Then solve: $\hat{\mathbf{p}} = \mathbf{p} - \frac{\delta t}{24}\left(V_\theta\left(\boldsymbol{\theta} + \delta t \mathbf{M}^{-1}\hat{\mathbf{p}}\right) - V_\theta\left(\boldsymbol{\theta} - \delta t \mathbf{M}^{-1}\hat{\mathbf{p}}\right)\right)$	Accept $(\boldsymbol{\theta}^*, \mathbf{p}^*)$ with probability $\min\left(1, \exp\left\{-\beta_B \Delta \tilde{H}\right\}\right)$.	The observable B is given by: $\langle B \rangle = \frac{\sum_{i=1}^{Ns} B.a_i}{\sum_{i=1}^{Ns} a_i}$, where $a_i = \frac{\exp(-\beta_B H(\boldsymbol{\theta}, \mathbf{p}))}{\exp(-\beta_B \tilde{H}(\boldsymbol{\theta}, \mathbf{p}))}$

Finally, in order to calculate balanced values of the mean, the results must be reweighted. This can be done using $f\left(\boldsymbol{\theta}, \boldsymbol{p}\right) / \hat{f}\left(\boldsymbol{\theta}, \boldsymbol{p}\right)$ before evaluating the averages. The average of an observable A is given by Equation (20). If the weighted vector parameter is described by $\tilde{\boldsymbol{\theta}}$, the mean value of the estimated parameters is given by:

$$\hat{\tilde{\boldsymbol{\theta}}} = E\left(\tilde{\boldsymbol{\theta}}\right) \cong \frac{1}{N_s} \sum_{i=1}^{N_s} \tilde{\boldsymbol{\theta}}^{\boldsymbol{i}} \tag{21}$$

where $\tilde{\boldsymbol{\theta}} = \frac{\boldsymbol{\theta} \cdot a_i}{\sum_{i=1}^{Ns} a_i}$ and $\boldsymbol{\theta}$ is the un-weighted uncertain vector. The mean value can be written as

$$\hat{\tilde{\boldsymbol{\theta}}} \cong \frac{1}{N_s} \sum_{i=1}^{N_s} \frac{a_i}{\sum_{j=1}^{Ns} a_j} \tilde{\boldsymbol{\theta}}^{\boldsymbol{i}} = \frac{1}{\sum_{j=1}^{Ns} a_j} \frac{1}{N_s} \sum_{i=1}^{N_s} a_i \boldsymbol{\theta}^{\boldsymbol{i}} = \frac{1}{\sum_{j=1}^{Ns} a_j} E\left(\boldsymbol{\theta}.\boldsymbol{a}^{\boldsymbol{T}}\right) \tag{22}$$

By following the same logic, the variance of the weighted estimated parameters is

$$V\left(\tilde{\boldsymbol{\theta}}\right) = E\left(\left(\tilde{\boldsymbol{\theta}} - \hat{\tilde{\boldsymbol{\theta}}}\right)^2\right) \cong V(\boldsymbol{\theta}). \frac{\sum_{i=1}^{Ns} a_i^2}{\left(\sum_{j=1}^{Ns} a_j\right)^2} \tag{23}$$

where $V(\boldsymbol{\theta})$ is the un-weighted variance, which is similar to the value estimated by the HMC algorithm (see Equation (14)), and the standard deviation is given by $\boldsymbol{\sigma}_{\tilde{\theta}} = \sqrt{V\left(\tilde{\boldsymbol{\theta}}\right)}$.

Table 1 summarizes the S2HMC algorithm, along with the HMC and SHMC algorithms. The differences between the procedures of sampling momentum along with the MD procedure are highlighted. The function $H_{[2k]}\left(\boldsymbol{\theta}, \boldsymbol{p}\right)$ represents the accurate shadow Hamiltonian of order k.

According to Table 1, the HMC algorithm is the easiest algorithm to programme, while the S2HMC algorithm requires a more complicated procedure to sample new momentum vectors than both the HMC and SHMC algorithms. The SHMC algorithm also requires a constant c to balance the acceptance rate of both the MD and MC steps.

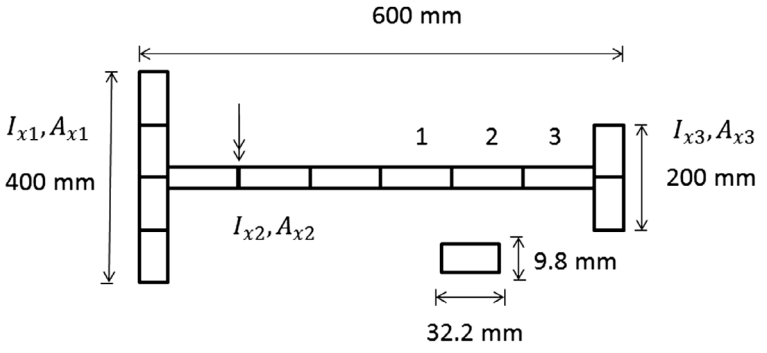

Figure 1. The H-shaped aluminium structure.

The MC and MD steps are both dependent on the parameter c (see Table 1). When c is large and positive, the SHMC algorithm becomes the HMC algorithm with different momentum vectors and this decreases the MD step acceptance rate (in the case that δt and/or system size are large). Otherwise, the MC step acceptance rate increases. A large negative c value increases the acceptance rate of the MD step and decreases the acceptance rate of the MC step. In this work, the original algorithm is modified so that the value of c is chosen to be proportional to the average difference between the Hamiltonian and the shadow Hamiltonian, which can be done offline as follows (the same strategy used in [27]):

(1) Run the SHMC between 50 and 100 iterations and save $\Delta H = H_{[2k]}(\boldsymbol{\theta}, \boldsymbol{p}) - H(\boldsymbol{\theta}, \mathbf{p})$ in a vector for all iterations.
(2) Determine the expected value $\overline{\Delta H}$ and standard deviation $\sigma_{\Delta H}$ for the obtained vector.
(3) Choose $c = \overline{\Delta H} - 1.2 \times \sigma^2_{\Delta H}$.

In the next sections, two structures are used to test the applicability of the S2HMC techniques to predict the uncertain parameters along with their errors. The structures are an unsymmetrical H-shaped beam structure and the GARTEUR SM-AG19 aeroplane structure. The results obtained by the S2HMC algorithms will be compared with those obtained by the HMC and SHMC algorithms. Since the S2HMC algorithm uses a fourth-order shadow Hamiltonian function, the results obtained with this algorithm are compared with the fourth-order SHMC (SHMC^4) results.

5. Unsymmetrical H-shaped structure

In this section, the un-symmetrical H-shaped aluminium structure (see Figure 1) is updated using the S2HMC algorithm. These results are compared with those obtained by the HMC and SHMC algorithms that were published in [27]. The SDT Matlab® package is used to model the structure. The original structure is divided into 12 elements and each single element is modelled as an Euler–Bernoulli beam. The double arrow in Figure 1 shows the location where the beam was excited using an electromagnetic shaker, while the acceleration was measured at 15 different positions. The response was measured by a roving accelerometer (see [4] for more details about the structure and the experiment).

Table 2. Initial and updated parameters using HMC, fourth-order SHMC and S2HMC.

	Initial $\boldsymbol{\theta}_0$	$\boldsymbol{\theta}$ vector, HMC Method	$\frac{\sigma_i}{\theta_i}$ (%)	$\boldsymbol{\theta}$ vector, SHMC Method	$\frac{\sigma_i}{\theta_i}$ (%)	$\boldsymbol{\theta}$ vector, S2HMC Method	$\frac{\sigma_i}{\theta_i}$ (%) =
I_{x1}	2.73×10^{-8}	2.21×10^{-8}	12.67	2.18×10^{-8}	12.60	2.19×10^{-8}	13.44
I_{x2}	2.73×10^{-8}	2.6×10^{-8}	1.37	2.49×10^{-8}	3.99	2.44×10^{-8}	2.70
I_{x3}	2.73×10^{-8}	2.9×10^{-8}	16.5	2.96×10^{-8}	14.93	2.95×10^{-8}	13.31
A_{x1}	3.16×10^{-4}	4.0×10^{-4}	1.39	4.05×10^{-4}	2.19	3.91×10^{-4}	2.93
A_{x2}	3.16×10^{-4}	2.3×10^{-4}	1.1	2.46×10^{-4}	2.10	2.34×10^{-4}	2.51
A_{x3}	3.16×10^{-4}	2.4×10^{-4}	1.95	2.25×10^{-4}	3.20	2.21×10^{-4}	7.44

5.1. H-beam simulation

The experimental natural frequencies are: 53.9, 117.3, 208.4, 254.0 and 445.0 Hz. In this paper, six uncertain parameters are updated, namely: the moments of inertia and the cross-sectional areas of each subsection of the beam (as shown in Figure 1). The unknown parameter vector is given by $\boldsymbol{\theta} = \{I_{x1}, I_{x2}, I_{x3}, A_{x1}, A_{x2}, A_{x3}\}$. The beam has the following structure parameters: Young's modulus is equal to 7.2×10^{10} N/m^2, the density of the material is set to 2785 kg/m^3 while the length and thickness of the beams are described in Figure 1. The set of updating parameters and the boundaries of the updated parameters are similar to those given in [27].

The posterior distribution function had the following constants: the temperature $T = 300$K, $\beta_B = \frac{1}{K_B 300}$ where $K_B = 0.00198719$ k cal mol^{-1}K^{-1}. The constant β_c of the posterior is set to 10, and the coefficients α_j are set equal to $\frac{1}{\sigma_j^2}$, where σ_j^2 is the variance of the jth parameter and the variance vector is defined as $\boldsymbol{\sigma} = \left[5\times10^{-8}, 5\times10^{-8}, 5\times10^{-8}, 5\times10^{-4}, 5\times10^{-4}, 5\times10^{-4}\right]$. These uncertain parameters are represented by a Gaussian distribution with a mean value equal to $\boldsymbol{\theta}_0$, and a variance $\boldsymbol{\sigma}$. To obtain a fast convergence of the algorithms, the constants of the prior (β_c and $\boldsymbol{\sigma}$) are chosen so that the weight of the likelihood terms will be greater than the prior terms in Equation (4). To keep our uncertain parameters physically realistic, maximum and minimum vectors are needed to bound the updated parameters. The maximum vector is $\left[3.73\times10^{-8}, 3.73\times10^{-8}, 3.73\times10^{-8}, 4.16\times10^{-4}, 4.16\times10^{-4}, 4.16\times10^{-4}\right]$ and the minimum vector is $\left[1.7\times10^{-8}, 1.7\times10^{-8}, 1.7\times10^{-8}, 2\times10^{-4}, 2\times10^{-4}, 2\times10^{-4}\right]$.

The number of samples is $N_s = 1000$, the initial time step is $\delta t = 0.0045$ s and the constant L is uniformly distributed on the interval.[1,10] To be certain of the results, each algorithm is implemented over 20 independent runs. The final results, tabulated in Tables 2 and 3, are the averages of these 20 runs, and these can accurately describe the results since a different momentum vector was used for each algorithm run.

Figure 2 represents the scatter plots with marginal histograms for four of the uncertain parameters using the S2HMC algorithm. In these figures, θ_i refers to the sequential numbering of the updating parameters in the updating vector, e.g. $\theta_2 = I_{x2}$ which is the second moment of area of the middle beam, and the normalization constants θ_i^0 are the initial (mean) values of the updated parameters. The plots show that the scatter is concentrated in a specific region, which means that the algorithm has found the region of high probability (which is almost the same as the HMC and SHMC algorithms in [27]). The expected values of the rest of the parameters along with their coefficient of variation (c.o.v) are given in Table 2.

Table 2 presents the initial and the updated values of the uncertain parameters. It also shows the coefficient of variation of the parameters for the S2HMC algorithm. The coefficient

Table 3. Natural frequencies and errors when HMC, SHMC and S2HMC are used to update the parameters.

Mode	Measured Frequency (Hz)	Initial Frequency (Hz)	Error (%)	Frequencies HMC Method (Hz)	Error (%)	Frequencies SHMC Method (Hz)	Error (%)	Frequencies S2HMC Method (Hz)	Error (%)
1	53.9	51.40	4.63	52.93 (0.17%)	1.8	52.94 (0.04%)	1.79	53.16 (0.83%)	1.37
2	117.3	116.61	0.59	118.82 (0.21%)	1.3	118.23 (0.15%)	0.79	118.78 (0.87%)	1.27
3	208.4	201.27	3.42	208.81 (0.24%)	0.2	207.91 (0.27%)	0.23	208.56 (0.99%)	0.078
4	254.0	247.42	2.59	254.41 (0.22%)	0.16	253.84 (0.17%)	0.06	254.04 (1.20%)	0.016
5	445	390.33	12.28	444.13 (0.41%)	0.2	443.0 (0.20%)	0.45	444.16 (1.56%)	0.19
Total average error	_____	_____	4.70	_____	0.73	_____	0.66	_____	0.58

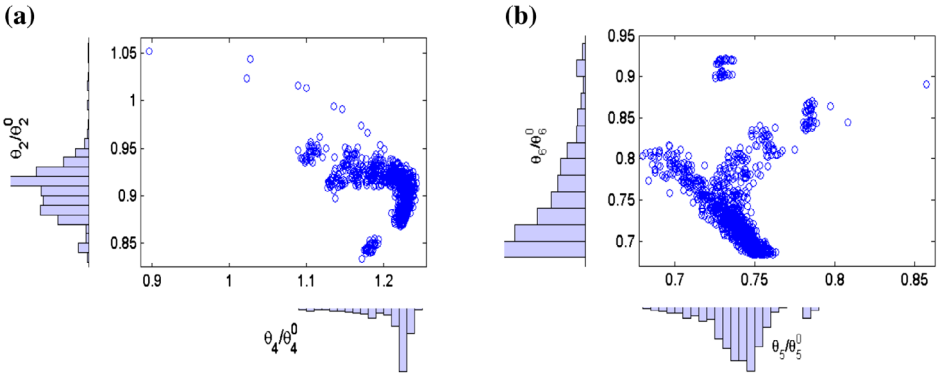

Figure 2. Scatter plots with marginal histograms, using the S2HMC method: (a) A_{x1} vs. I_{x2} (b) A_{x2} vs. A_{x3}.

of variation (c.o.v) represents the percentage of estimated standard deviation divided by the estimated $\boldsymbol{\theta}$ for each algorithm: $\frac{\sigma_i}{\theta_i}$ (%). The results obtained by the HMC and SHMC algorithms in [27] are also presented in Table 2. The estimate of the middle beam parameters, particularly the second moment of area, is more accurate than the left and the right beam parameters, which can be seen from the values of the coefficient of variation in Table 2. The strain in the lower modes will be higher in the middle beam, meaning that the lower natural frequencies are more sensitive to the stiffness of the middle beam. The same observation is made when the HMC and SHMC algorithms are employed to update the same structure.

In general, the S2HMC algorithm updated $\boldsymbol{\theta}$ vector which is physically realistic. The time step used provides a very good sampling acceptance rate for all algorithms (99.9%). The updated values and the coefficient of variation for the HMC and SHMC algorithms found in [27] are close to those obtained by the S2HMC algorithm.

Table 3 presents the updated natural frequencies for each mode, the absolute mode errors and the final model error in percentages for all three algorithms. The coefficient of variation is given in the parenthesis and represents the estimated standard deviation divided by the estimated frequency. The absolute mode errors are given by $\frac{|f_i^m - f_i^a|}{f_i^m}$, while the total average error, or the sum of the mode errors, (TAE) is given by $\text{TAE} = \frac{1}{N_m}\sum_{i=1}^{N_m}\frac{|f_i^m - f_i^a|}{f_i^m}$. The main goal of the updating process is to improve the analytical frequencies by reducing the total average error; hence, the errors in all of the individual modes are not necessarily simultaneously reduced. The constant β_c in Equation (4), which is used to weight the likelihood terms in the posterior, can be selected as a vector to improve certain modes. However, increasing the weight for certain frequencies does not guarantee the improvement of all modes and the TAE value.

Different methods have been used to update the H-shaped beam structure. The Nelder Mead (NM) simplex method reduced the error to 2.14% in [4], while the response surface (RS) method [4] produced a total average error of 1.84% in [4]. Both the HMC and SHMC algorithms were applied to update the same structure and the HMC algorithm reduced the error to 0.73%, while the fourth-order SHMC algorithm reduced the error to 0.66% (both the HMC and SHMC results obtained in [27] are presented in Table 3).

From Table 3, the error between the first measured natural frequency and that of the initial model was 4.63%. When the S2HMC algorithm was applied, the error decreased to

1.37%. The same comments can be made for the third, fourth and fifth natural frequencies. Overall, the updated FEM natural frequencies for the S2HMC algorithm are better than the initial FEM.

When results obtained by the S2HMC algorithm are compared to those obtained by both the HMC and SHMC algorithms, the S2HMC algorithm produced a slightly better total average error result than both the HMC and SHMC algorithms. The updating using the S2HMC method reduced the total average error from 4.7 to 0.58%, which is an acceptable percentage since the error is smaller than that obtained by the NM, RS, HMC and SHMC methods.

The coefficient of variation (c.o.v) for the S2HMC algorithms is very small. This indicates that the updating process using the separable shadow Hamiltonian algorithm under the Bayesian approach produced accurate results.

Figure 3 shows the correlation between all of the updated parameters. Smaller values indicate that the parameters are weakly correlated (<0.3). Large values (>0.7) indicate that the parameters are highly correlated, while zero indicates that the parameters are not correlated. A positive correlation means that the variables are positively related, while a negative correlation indicates the opposite. Figure 3 shows that all parameters (except A_{x1}vs. A_{x3}) are weakly correlated. The pair (A_{x1}, A_{x3}) is highly correlated (the correlation is equal to 0.71).

The convergence of the total average error over a number of iterations is shown in Figure 4. The y-axis (Total Average Error) is defined on a logarithmic scale, while the x-axis represents the iterations of the S2HMC algorithm. To obtain this figure, the previously accepted samples are used to compute the mean at every iteration i ($\hat{\boldsymbol{\theta}} = E(\boldsymbol{\theta}) \cong \frac{1}{N_s}\sum_{j=1}^{i} \boldsymbol{\theta}^{\boldsymbol{i}}$ where i represents the current iteration). Then, the total average error is computed according to $\mathrm{TAE(i)} = \frac{1}{i}\sum_{j=1}^{N_m} \frac{|f_j^m - f_j|}{f_j^m}$. The results obtained by the S2HMC are compared in the same plot with those obtained in [27] using the HMC and SHMC algorithms. The S2HMC algorithm converges fast and within the first 100 iterations, and has similar properties to the SHMC algorithm when the time step is relatively small. The HMC converges more slowly, but even in this case, 200 iterations (or 200 samples) would be sufficient to have good updated parameters.

The time step used in the Hamiltonian algorithms determines the accuracy of these algorithms. Figure 5 shows the sampling acceptance rate (AR) of the HMC, SHMC and S2HMC algorithms when the time step varies between 0.006 and 0.01 s. The S2HMC algorithm has extended the upper boundary of the HMC time step. The S2HMC method maintains a good acceptance rate when the time step is increased. At time step 0.006 s, the S2HMC algorithm has an acceptance rate equal to 99.9%. The S2HMC algorithm preserves the same AR value until δt = 0.0066 s, and then the AR of the algorithm starts decreasing from δt = 0.0068 s (AR equal to 93.3%) to reach an acceptance rate equal to 69.7% at time step δt = 0.01 s. At time step δt = 0.01 s, the S2HMC algorithm achieves an acceptance rate slightly better than the SHMC acceptance rate (66% for the SHMC algorithm), while the AR of the HMC algorithm at time step δt = 0.01 s is less than 1% (no samples were accepted).

Figures 4 and 5 show that the results of the S2HMC and SHMC algorithms are close in terms of convergence and acceptance rates. However, the average running time (computational time to run the algorithm) for HMC, SHMC (4th order) and S2HMC algorithms for 1000 iterations is: 28.63, 89.33 and 43.12 min, respectively. The running time for the HMC algorithm is less than both SHMC and S2HMC since there are no complexities in its

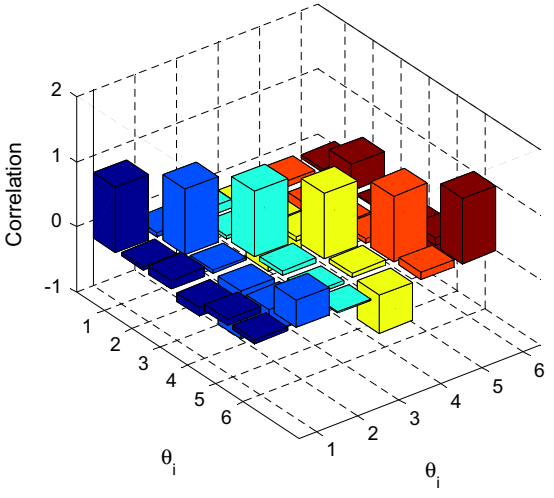

Figure 3. The correlation between the updated parameters (S2HMC algorithm).

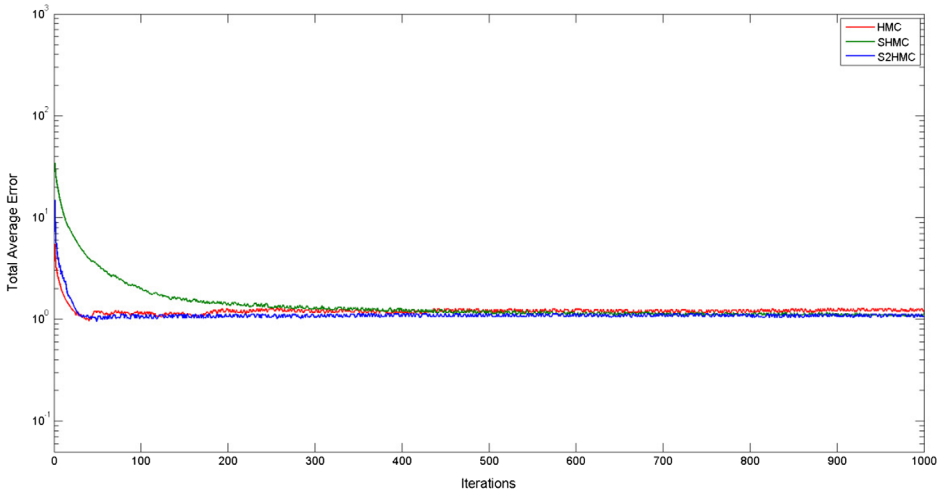

Figure 4. The convergence of the HMC, SHMC and S2HMC methods.

MC and MD steps (see Table 1). The S2HMC algorithm does have a relatively large time step since it requires evaluating the separable shadow Hamiltonian function. On the other hand, the SHMC algorithm has a longer running time since both MC and MD steps require accept–reject procedure to accept samples. Table 1 indicates that the SHMC has a complicated procedure to obtain new momentum values. Figure 6 describes both the MC and MD procedures of the SHMC algorithm when the constant c varies between 0.001 and 1. The constant c plays a very important role in SHMC algorithm since the acceptance rate of both MC and MD steps can be balanced using this constant. The constant c should be small to have a better acceptance rate in the MD step, but at the same time, the value of c should be large enough to have a good acceptance rate when the momentum is sampled (MC step). The MC acceptance rate started at 28% when $c = 0.001$, which is not a good AR, since the

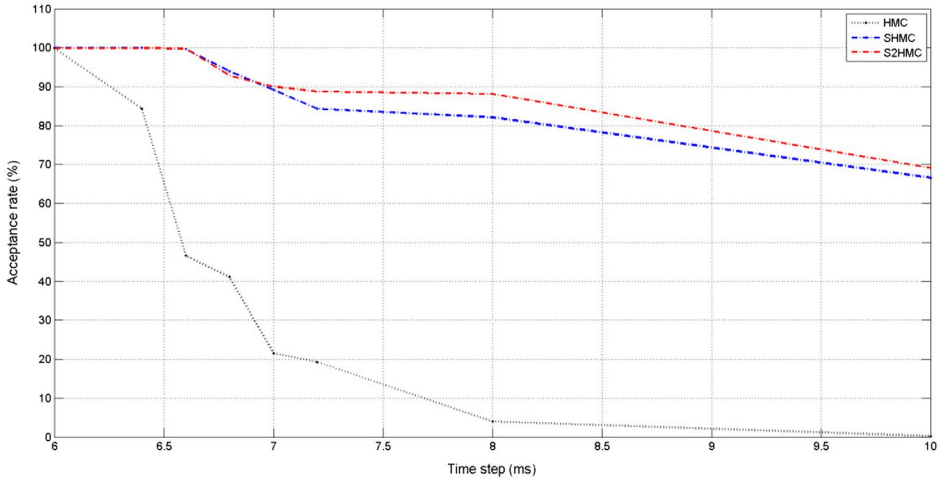

Figure 5. The acceptance rate obtained for different time steps using the HMC, SHMC and S2HMC algorithms.

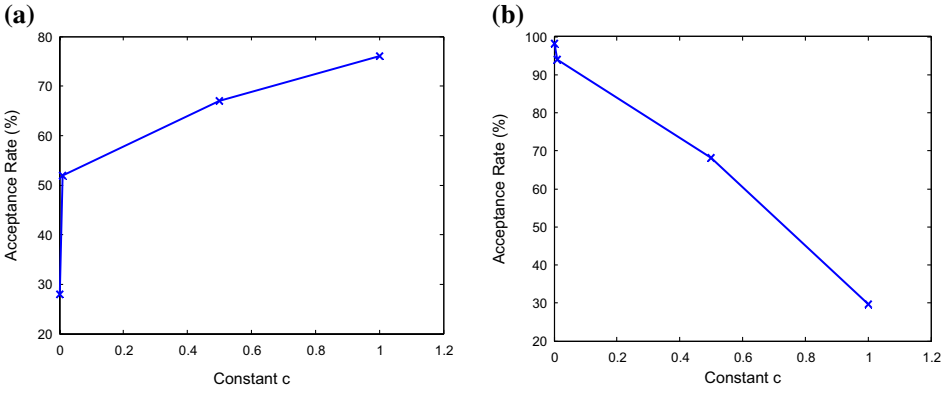

Figure 6. The MD and MC acceptance rate of the SHMC algorithm when ***c*** varies: (a) MC acceptance rate and (b) MD acceptance rate.

algorithm needs more time to produce new momentum, while the AR reached 76% when $c = 1$. In contrast, the MD acceptance rate started very high at 98.1% when $c = 0.001$ and decreases to 29.6% when $c = 1$. The SHMC algorithm used a constant $c = 0.01$, which indicates that the MC step had an AR equal to 52%. On the other hand, the S2HMC algorithm has a very simple momentum sampling procedure since all momentum samples will be accepted without the use of any extra constant and this can reduce the iterations of the algorithm (the S2HMC algorithm's computation cost is less than the SHMC algorithm's cost).

The results from Tables 2 and 3 do not conclusively determine which Monte Carlo algorithm is better for this relatively simple FEM problem. To explore this issue further, a more complex structure is considered in the next section. In general, one single implementation is not sufficient to reach any conclusions about the relative performance of the HMC, SHMC and S2HMC methods. In this case, a second implementation using a complicated system is needed to study the efficiency and the limitations of the algorithms.

Figure 7. The GARTEUR SM-AG19 structure. This picture is reproduced with permission from the Department of Flight Mechanics, Flight Control and Aeroelasticity, TU Berlin, Germany (www.fmra.tu-berlin.de).

6. The GARTEUR SM-AG19 structure

In this section, the GARTEUR SM-AG19 structure [38–43] is updated using the S2HMC algorithm. The results obtained are compared with those obtained in [27] where the same set of parameters and boundaries are used. The GARTEUR SM-AG19 structure is shown in Figure 7.[39]

This structure has been updated, using different sets of uncertain parameters. More details about the methods used to update the structure can be found in [43], where Link and Friswell summarized the results obtained by seven participants. The updating procedures were performed differently. Each participant used a different set of uncertain parameters and many computational methods were tested in this structure. The participants obtained different total average errors that varied between 0.69 and 2.03%. The structure has also been modified in different studies where a mass was added to both wings, and the average errors were reduced to values between 1.02 and 1.50%.

The structure has the following characteristics: length of the fuselage is 1.5 m, the wingspan is 3 m and the depth of the fuselage is equal to 15 cm, while the thickness is 5 cm. The structure is made of aluminium and its mass is 44 kg. A $1.1 \times 76.2 \times 1700\,\text{mm}^3$ viscoelastic constraining layer was bonded to the wings to increase the damping. Further details are described in Refs. [39,43]. In the models used for this research, all element materials are considered to be standard isotropic. The model elements are Euler–Bernoulli beam elements.

6.1. GARTEUR simulation

The experimental test data used were those obtained from DLR Göttingen, Germany. The measured natural frequencies (Hz) are: 6.38, 16.10, 33.13, 33.53, 35.65, 48.38, 49.43, 55.08, 63.04 and 66.52 Hz. The parameters of the structure to be updated are the right wing moments of inertia and torsional stiffness ($R\backslash I_{\text{min}}$, $R\backslash I_{\text{max}}$, $R\backslash I_{\text{tors}}$), the left wing moments of inertia and torsional stiffness ($L\backslash I_{\text{min}}$, $L\backslash I_{\text{max}}$, $L\backslash I_{\text{tors}}$), the vertical tail moment of inertia ($VTP\backslash I_{\text{min}}$) and the overall mass density of the structure ρ.

Table 4. The initial values of the updating parameters for the GARTEUR example.

Parameter	ρ (kg/m^3)	$VTP\_I_{\min}$ (10^{-9}m^4)	$L\_I_{\min}$ (10^{-9}m^4)	$L\_I_{\max} b$
	2785	8.34	8.34	8.34
Parameter	L_I_{tors}(10^{-8}m^4)	$R\_I_{\min}$ (10^{-9}m^4)	$R\_I_{\max}$ (10^{-7}m^4)	R_I_{tors} (10^{-8}m^4)
	4.0	8.34	8.34	4.0

Table 5. The bounds of the updating parameters for the GARTEUR example.

	Max	Min
ρ	3500	2500
$VTP\_I_{\min}$	12×10^{-9}	5×10^{-9}
$L\_I_{\min}$	12×10^{-9}	5×10^{-9}
$L\_I_{\max}$	12×10^{-7}	5×10^{-7}
$R\_I_{\min}$	12×10^{-9}	5×10^{-9}
$R\_I_{\max}$	12×10^{-7}	5×10^{-7}
L_I_{tors}	6×10^{-8}	3×10^{-8}
R_I_{tors}	6×10^{-8}	3×10^{-8}

The temperature $T = 300\,\text{K}$, $\beta_B = \frac{1}{K_B 300}$ where $K_B = 0.00198719\,\text{kcal mol}^{-1}\text{K}^{-1}$. The update vector is given by $\boldsymbol{\theta} = [\rho, VTP\_I_{\min}, L\_I_{\min}, L\_I_{\max}, R\_I_{\min}, R\_I_{\max}, L\_I_{tors}, R\_I_{tors}]$. The Young's modulus for the aeroplane is set to 7.2×10^{10} N/m^2. In Equation (6), the constant β_c of the posterior distribution is set equal to 100. All coefficients α_j are set equal to $\frac{1}{\sigma_j^2}$, where σ_j^2 is the variance of the jth parameter and $\boldsymbol{\sigma} = \left[5 \times 10^2, 5 \times 10^{-9}, 5 \times 10^{-9}, 5 \times 10^{-7}, 5 \times 10^{-9}, 5 \times 10^{-7}, 5 \times 10^{-8}, 5 \times 10^{-8}\right]$.

The mean values of the updated vector and their bounds are given in Tables 4 and 5, respectively. The bounds of the updated parameters are different from those in Ref. [29]; the bounds were increased to avoid obtaining results close to these bounds and the new bounds in Table 5 gave better results than those obtained in [29]. The time step is set to $\delta t = 3$ ms and the number of samples is $N_s = 1000$. Each algorithm was run over 10 independent simulations. The final results tabulated in Tables 6 and 7 are the averages of these 10 runs.

In this study, the S2HMC algorithm is implemented to update the FEM of the above structure and the results obtained are compared to those obtained by the SHMC and HMC algorithms.[27] Again, in this example, the same comments can be made for the computational time for the three algorithms where the average running time for HMC, SHMC (fourth order) and S2HMC algorithms for 1000 iterations is: 82.81, 167.44 and 107.63 min, respectively. Table 6 presents the initial values (the means of the material or geometric parameters) of the updating vector $\boldsymbol{\theta}$, the updated values and the corresponding coefficient of variation (c.o.v) obtained by the S2HMC, HMC and the SHMC methods for two time steps.

When the time step is $\delta t = 0.003$ s, the S2HMC algorithm updated all parameters and the precision of these updated parameters is considered good since the coefficients of variation for all parameters are small. The time step used is relatively small, which might mean that the HMC algorithm has more advantages than the SHMC and S2HMC algorithms. This can be seen in the c.o.v values. The HMC c.o.v values are smaller than both the SHMC and S2HMC results (Table 6). In general, c.o.v values are small for the updated parameters when the three Hamiltonian algorithms are implemented to update the structure (smaller

Table 6. Initial and updated parameter values for the HMC, SHMC and S2HMC algorithms.

	Initial (the mean vector) θ_0	HMC Method $\delta t = 3\,\text{ms}\,\theta$	$\frac{\sigma_i}{\mu_i}$ (%) c.o.v	SHMC[4] Method $\delta t = 3\,\text{ms}\,\theta$	$\frac{\sigma_i}{\mu_i}$ (%) c.o.v	S2HMC Method $\delta t = 3\,\text{ms}\,\theta$	$\frac{\sigma_i}{\mu_i}$ (%) c.o.v	SHMC Method $\delta t = 4.8\,\text{ms}\,\theta$	$\frac{\sigma_i}{\mu_i}$ (%) c.o.v	S2HMC Method $\delta t = 4.8\,\text{ms}\,\theta$	$\frac{\sigma_i}{\mu_i}$ (%) c.o.v
ρ	2785	2667.33	1.97	2666.85	2.27	2732.4	2.39	2737.66	3.42	2764.2	2.24
$VTP\backslash_{min}$	8.34×10^{-9}	6.938×10^{-9}	5.62	6.961×10^{-9}	5.50	7.18×10^{-9}	6.20	7.467×10^{-9}	10.54	7.25×10^{-9}	4.49
$L\backslash_{min}$	8.34×10^{-9}	10.12×10^{-9}	2.34	10.12×10^{-9}	2.27	10.42×10^{-9}	3.12	10.15×10^{-9}	1.63	10.52×10^{-9}	1.96
$L\backslash_{max}$	8.34×10^{-7}	7.899×10^{-7}	2.61	7.919×10^{-7}	2.75	8.134×10^{-7}	2.29	8.184×10^{-7}	2.93	8.206×10^{-7}	2.48
$R\backslash_{min}$	8.34×10^{-9}	10.15×10^{-9}	2.13	10.13×10^{-9}	2.21	10.13×10^{-9}	2.50	10.14×10^{-9}	1.52	10.17×10^{-9}	1.37
$R\backslash_{max}$	8.34×10^{-7}	6.11×10^{-7}	3.14	6.096×10^{-7}	4.02	6.102×10^{-7}	4.34	6.305×10^{-7}	2.30	6.085×10^{-7}	2.30
$L\backslash_{tors}$	4×10^{-8}	4.043×10^{-8}	1.95	4.036×10^{-8}	2.09	4.037×10^{-8}	1.62	3.969×10^{-8}	3.24	4.039×10^{-8}	1.79
$R\backslash_{tors}$	4×10^{-8}	3.571×10^{-8}	2.17	3.563×10^{-8}	2.49	3.565×10^{-8}	2.09	3.623×10^{-8}	1.81	3.574×10^{-8}	1.80

Table 7. Modal results and errors for S2HMC method at two different time steps.

Mode	Measured Frequency (Hz)	Initial FEM Frequencies (Hz)	Error (%)	Frequencies HMC Method (Hz) $\delta t = 3$ ms	Error (%)	SHMC Frequencies (Hz) $\delta t = 3$ms	Error (%)	Frequencies S2HMC Method (Hz) $\delta t = 3$ ms	Error (%)	Frequencies SHMC Method (Hz) $\delta t = 4.8$ ms	Error (%)	Frequencies S2HMC Method (Hz) $\delta t = 4.8$ ms	Error (%)
1	6.38	5.71	10.47	6.313 (0.95%)	1.06	6.312 (1.30%)	1.07	06.326 (1.34%)	0.85	6.284 (2.06%)	1.50	06.334 (0.92%)	0.74
2	16.10	15.29	5.01	15.866 (0.81%)	1.45	15.875 (1.38%)	1.40	15.995 (0.84%)	0.65	16.043 (2.19%)	0.35	16.037 (0.93%)	0.39
v3	33.13	32.53	1.82	32.236 (0.75%)	2.70	32.238 (1.43%)	2.69	32.290 (0.72%)	2.54	32.453 (2.26%)	2.04	32.307 (0.75%)	2.48
4	33.53	34.95	4.23	33.90 (0.76%)	1.10	33.88 (1.52%)	1.04	33.906 (0.63%)	1.11	33.991 (2.4%)	1.38	33.929 (0.75%)	1.19
5	35.65	35.65	0.0117	35.643 (0.31%)	0.02	35.62 (1.45%)	0.083	35.609 (0.42%)	0.12	35.517 (2.30%)	0.37	35.606 (0.67%)	0.12
6	48.38	45.14	6.69	48.84 (0.61%)	0.95	48.80 (1.36%)	0.87	48.599 (0.71%)	0.45	48.879 (2.15%)	1.03	48.434 (0.73%)	0.11
7	49.43	54.69	10.65	49.871 (1.45%)	0.89	49.86 (1.61%)	0.88	49.706 (1.47%)	0.56	49.367 (2.55%)	0.13	49.630 (0.94%)	0.40
8	55.08	55.60	0.94	54.364 (0.83%)	1.30	54.418 (1.47%)	1.20	54.684 (0.76%)	0.72	55.093 (2.32%)	0.02	54.728 (0.93%)	0.64
9	63.04	60.15	4.59	63.888 (0.68%)	1.35	63.896 (1.39%)	1.36	63.827 (0.77%)	1.25	63.628 (2.19%)	0.93	63.773 (0.76%)	1.16
10	66.52	67.56	1.57	67.446 (0.029%)	1.39	67.447 (1.48%)	1.39	67.444 (0.26%)	1.39	67.458 (2.34%)	1.41	67.441 (0.54%)	1.38
Total average errors	_____	_____	4.6	_____	1.22	_____	1.20	_____	0.964	_____	0.92	_____	0.86

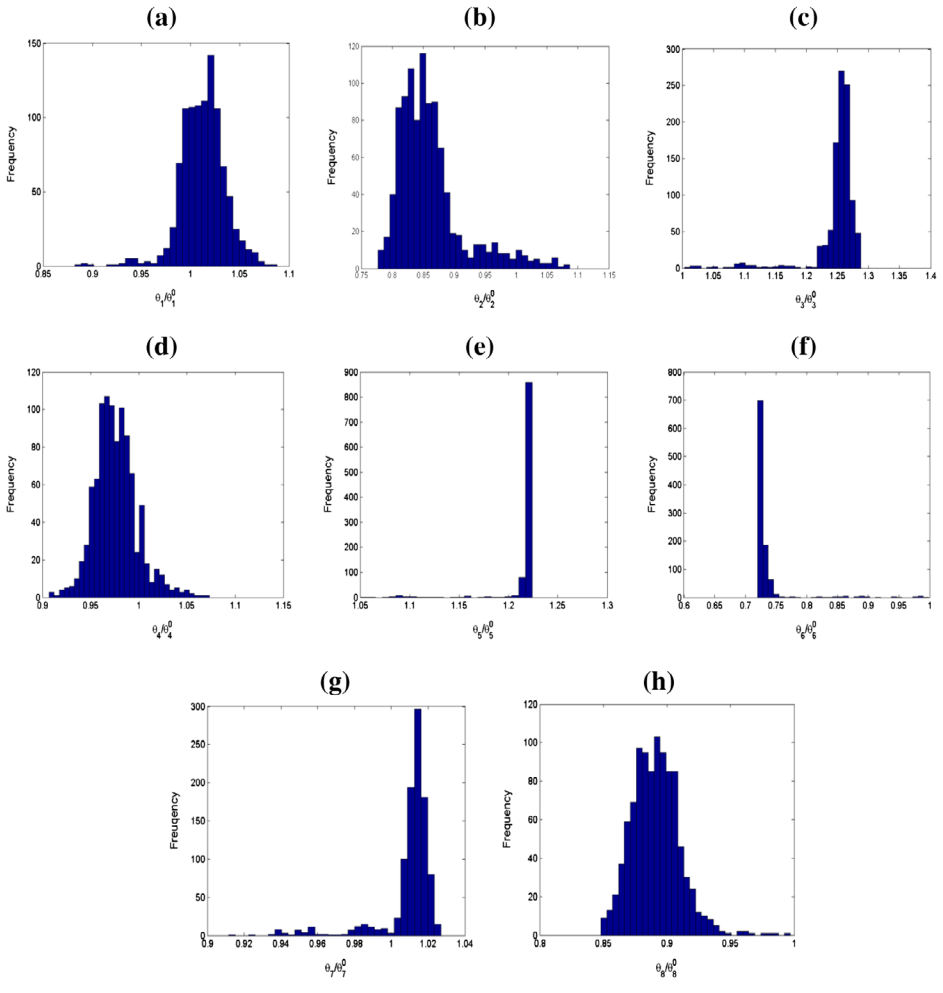

Figure 8. Histograms of updating model parameters using the S2HMC method. The normalization constants θ_4^0, θ_7^0 and θ_8^0 are the initial (mean) values: (a) ρ (b) $VTP\backslash V_{min}$ (c) $L\backslash V_{min}$ (d) $L\backslash V_{max}$ (e) $R\backslash V_{min}$ (f) $R\backslash V_{max}$ (g) $L\backslash V_{tors}$ (h) $R\backslash V_{tors}$.

than 6% for both the HMC and SHMC algorithms, and smaller than 6.5% for the S2HMC algorithm).

When a relatively large time step ($\delta t = 0.0048$ s) is used, the updated parameters obtained by the S2HMC method are much closer to the mean value than those obtained using a time step of $\delta t = 0.003$ s. In this setting, the HMC method gives poor updating parameters.[27] The updated and same initial parameters were identical since no new samples were accepted (see [27] for more details). The reason is that the Hamiltonian function rapidly fluctuated with time, and this caused a sudden decrease in the acceptance rate (the acceptance rate decreases to less than 1% when the time step is $\delta t = 0.0048$ s). The acceptance rates for the S2HMC and the SHMC algorithms are 71 and 70%, respectively, which is an acceptable rate compared to that of the HMC method. However, the S2HMC algorithm requires less implementation time than the SHMC algorithm. The constant $c = 0.01$ used in this example reduces the SHMC acceptance rate of the MC step to 61.2%, which indicates that the SHMC

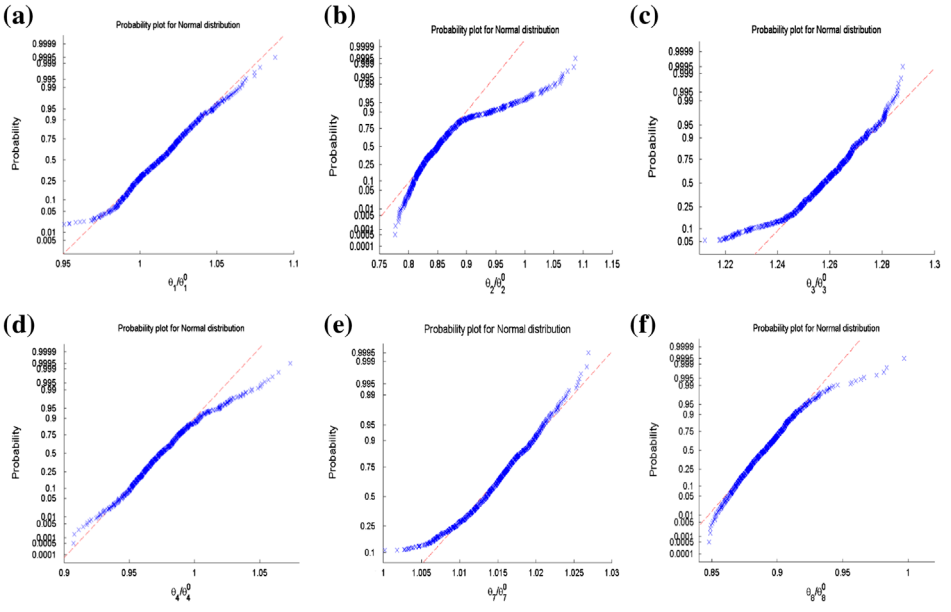

Figure 9. Normal probability plots for $L\backslash I_{max}(\theta_4)$, $L\backslash I_{tors}(\theta_7)$ and $R\_I_{tors}(\theta_8)$ from the S2HMC algorithm for the GARTEUR example. The straight line indicates a Gaussian distribution of data: (a) $L\backslash I_{max}$ (b) $L\backslash I_{tors}$ (c) $L\backslash I_{max}$ (d) $L\backslash I_{tors}$ (e) $R\backslash I_{tors}$ and (f) $R\backslash I_{tors}$.

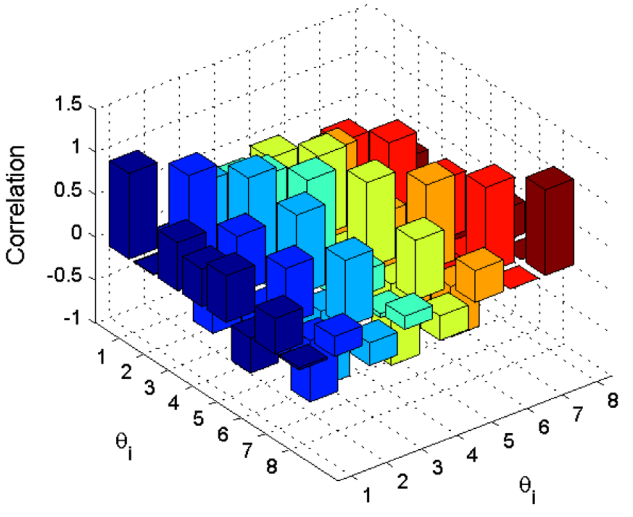

Figure 10. The correlation between the updated parameters (S2HMC algorithm).

algorithm takes a long time to sample momentum, while the S2HMC initially uses a similar approach as the HMC method to sample new momentum vectors, while the pre-processing step transforms the momentum to be evaluated to a different search space.

The time step $\delta t = 0.0048$ s allows the S2HMC algorithm to give slightly more precise results than those obtained by time step $\delta t = 0.003$ s. This can be verified from Table 6 where the c.o.v values obtained by the S2HMC algorithm when $\delta t = 0.0048$ s are smaller than

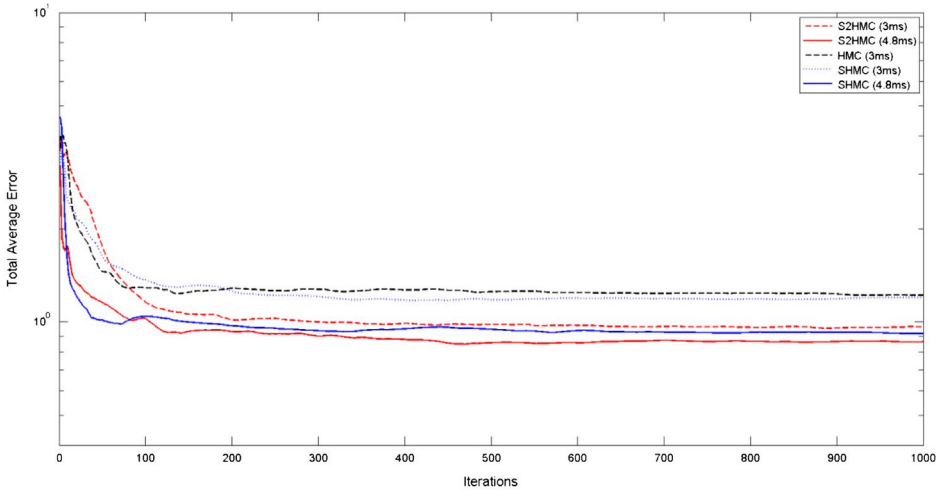

Figure 11. The total average error using the HMC, SHMC and S2HMC methods.

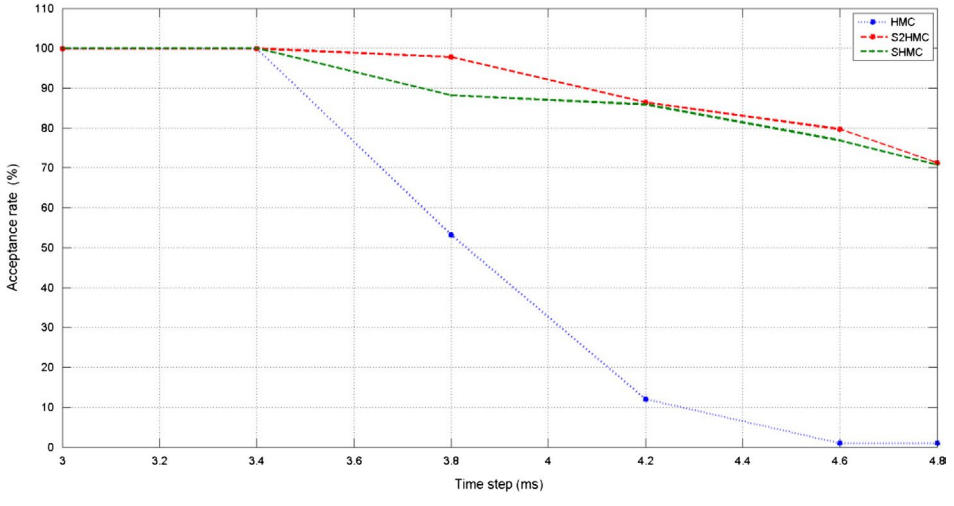

Figure 12. The acceptance rate obtained for different time steps using the HMC, SHMC and S2HMC methods.

those obtained by the same algorithm when $\delta t = 0.003$ s. Also, the c.o.v values obtained by the S2HMC algorithm are smaller than those obtained by the HMC and SHMC algorithms, which means that the S2HMC algorithm produced more accurate results than those obtained by the other two algorithms (the c.o.v values are less than 4.5% for S2HMC algorithm, while it reaches more than 10% for some parameters using the SHMC algorithm.).

Figure 8 presents the histograms of the updating parameters using the S2HMC method. In these figures, θ_i refers to the sequential numbering of the updating parameters in the updating vector, e.g. $\theta_1 = \rho$ (density), and the normalization constants θ_i^0 are the initial (mean) values of the updated parameters. The results show that the S2HMC algorithm

was successfully able to identify the high probability region (the density of the parameters varies over a very small region, especially those of θ_5 and θ_6.

It is noticeable that the density function of ρ, $VTP\backslash I_{\min}$, $L\backslash I_{\min}$, $L\backslash I_{\max}$, $L\backslash I_{\text{tors}}$ and $R\backslash I_{\text{tors}}$ has forms similar (or close) to normal distribution function forms, while the density of the other parameters has different forms. The Gaussian probability plots for these six updated parameters using the S2HMC algorithm are presented in Figure 9. The results verify that some of these six parameters have an almost Gaussian distribution, especially ρ, $L\backslash I_{\text{tors}}$ and $R\backslash I_{\text{tors}}$ (non-Gaussian behaviours are seen in tails of the plots).

Figure 10 shows the correlation between all of the updated parameters for the S2HMC algorithm. All of the parameters are correlated (no values are close to 0); the pairs ($L\backslash I_{\min}$, $R\_I_{\min}$), ($L\backslash I_{\min}$, $R\_I_{\max}$) and ($R\backslash I_{\max}$, $R\_I_{\min}$) are highly correlated, while the pairs (ρ, $R\_I_{\max}$), (ρ, $R\_I_{\min}$) and (ρ, L_I_{tors}) are weakly correlated.

Table 7 gives the updated natural frequencies and output errors when the S2HMC algorithm is employed. The results show that the updated FEM natural frequencies are better than the initial FEM using the S2HMC algorithm with both time steps. When $\delta t = 0.003$ s, the error between the first measured natural frequency and that of the initial model was 10.47%, and the S2HMC reduced the error to 0.85%. A similar observation can be made for the second, fourth, sixth, seventh, eighth and ninth natural frequencies. The initial total average error was 4.6%, but after using the S2HMC method, it was reduced to 0.964% (better than 1.22% obtained by HMC and 1.20% obtained by SHMC). In general, the updated natural frequencies obtained by the three algorithms are better than the initial structural modes, and this can be seen from the total average error in Table 7.

Figure 11 shows the total average error of the HMC, SHMC and S2HMC algorithms for both time steps over 1000 iterations. Similar to Figure 4, the y-axis, which represents the Total Average Error, is plotted using a logarithmic scale. The S2HMC algorithm converges fast and almost has the same convergence rate for both time steps (the algorithms start to converge in the first 100–150 iterations).

The time step $\delta t = 0.003$ s provides a good acceptance sampling rate for the S2HMC algorithm (99.9%). Choosing a different time step may reduce the acceptance sampling rate for this method. The time step can significantly affect the convergence rate and the results obtained, especially for those algorithms that use the original Hamiltonian function. In the case where the time step $\delta t = 0.0048$ s, the S2HMC method improves the total average error (TAE) and reduces the c.o.v values. This can be seen in Table 7 where the total average error is reduced to 0.68% with an acceptance rate of 71%. However, this is not the case for HMC, where the acceptance rate decreases to less than 1%. Using this time step, the updated vector obtained from the HMC does not improve the FEM results. So the advantage of the S2HMC algorithm is its ability to use a large time step, which is not the case with the HMC algorithm. This allows the S2HMC method to overcome the complexities of sampling the momentum vector. The updated modes are close for both SHMC and S2HMC algorithms since they both use the advantage of the gradient to converge to the same local optimal vector and both allow relatively large time steps. However, the S2HMC algorithm is faster than the SHMC algorithm since the SHMC algorithm is required to run an extra procedure (the MC step) to accept the new momentum.

Figure 12 shows the acceptance rate for different time steps. The acceptance rate of the S2HMC algorithm is 99.9% when the time step is 3 ms. The acceptance rate starts decreasing when the time step increases but this decrease is faster and more significant in the case of

the HMC method (similar to [27]). When the time step $\delta t = 3.4$ ms, the acceptance rate for the S2HMC is 99.9% and reduces slightly to 97.8% when the time step reaches 3.8 ms. Finally, when the time step is 4.8 ms, the S2HMC acceptance rate reduces to 71.3%, while SHMC algorithm has an AR equal to 70.8%, which is an acceptable rate compared to that obtained by the HMC method (less than 1%).

7. Conclusion

This paper analyses the applicability of three sampling techniques using the Bayesian formulation of the finite element model update problem. These methods are tested on two real-world structures: an unsymmetrical H-shaped beam and the GARTEUR SM-AG19 structure. These sampling methods are used to evaluate the posterior distribution function of Bayes' theorem for FEM updating. All these methods use the Markov Chain Monte Carlo (MCMC) type sampling approach. Of particular interest in this paper are the subtle differences in performance of these algorithms, the hybrid Monte Carlo, the shadow hybrid Monte Carlo and the separable shadow Hamiltonian Monte Carlo algorithm. The paper details these algorithms, highlights their parameters and their performance characteristics.

In both experiments, the results obtained by the S2HMC algorithm are better than both the SHMC and HMC algorithms. The resultant total average error of the updated model parameters is lower, the sampling acceptance rate is higher and the convergence of the S2HMC algorithm is faster. This is mainly due to the S2HMC algorithm being able to efficiently sample the search space at larger time steps and being faster in producing new momentum values. The use of the separable Hamiltonian is thus a useful modification to the classic hybrid Monte Carlo algorithm.

Disclosure statement

No potential conflict of interest was reported by the authors.

References

[1] Onãte E. Structural analysis with the finite element method. Linear Statics. Vol. 1, Basis and Solids. Dordrecht: Springer; 2009.
[2] Rao SS. The finite element method in engineering. 4th ed. Burlington, (VT): Elsevier Butterworth Heinemann; 2004.
[3] Friswell MI, Mottershead JE. Finite element model updating in structural dynamics. Dordrecht: Kluwer Academic; 1995.
[4] Marwala T. Finite-element-model updating using computional intelligence techniques. London: Springer Verlag; 2010.
[5] Yuen KV. Bayesian methods for structural dynamics and civil engineering. New York (NY): Wiley; 2010.
[6] Cheung SH, Beck JL. Bayesian model updating using hybrid Monte Carlo simulation with application to structural dynamic models with many uncertain parameters. J. Eng. Mech. 2009;135:243–255.
[7] Boulkaibet I, Marwala T, Mthembu L, et al. Sampling techniques in Bayesian finite element model updating. Proc. Soc. Exp. Mech. 2012;29:75–83.
[8] Marwala T, Sibisi S. Finite element model updating using Bayesian approach. In: Proceedings of the International Modal Analysis Conference; Orlando, FL; 2005. ISBN: 0-912053-89-5.

[9] Beck JL, Katafygiotis LS. Updating models and their uncertainties. I: Bayesian statistical framework. J. Eng. Mech. 1998;124:455–461.
[10] Haddad Khodaparast H. Stochastic finite element model updating and its application in aeroelasticity [PhD thesis]. Liverpool: University of Liverpool; 2010.
[11] McKay MD, Conover WJ, Beckman RJ. A comparison of three methods for selecting values of input variables in the analysis of output from a computer code. Technometrics. 1979;21:239–245.
[12] Koehler JR, Owen AB. Computer experiment. In: Ghosh S, Rao CR, editor. Handbook of statistics. Vol. 13. New York (NY): Elsevier-Science; 1996. p. 261–308.
[13] Bishop CM. Pattern recognition and machine learning. New York (NY): Springer-Verlag; 2006.
[14] Bishop CM. Neural networks for pattern recognition. Oxford: Oxford University Press; 1995.
[15] Metropolis N, Rosenbluth AW, Rosenbluth MN, et al. Equation of state calculations by fast computing machines. J. Chem. Phys. 1953;21:1087–1092.
[16] Hastings WK. Monte Carlo sampling methods using Markov chains and their applications. Biometrika. 1970;57:97–109.
[17] Au SK, Beck JL. Important sampling in high dimensions. Struct. Saf. 2003;25:139–163.
[18] Ching J, Muto M, Beck JL. Structural model updating and health monitoring with incomplete modal data using gibbs sampler. Comput. Aided Civ. Infrastruct. Eng. 2006;21:242–257.
[19] Geman S, Geman D. Stochastic relaxation, Gibbs distributions, and the Bayesian restoration of images. IEEE Trans. Pattern Anal. Mach. Intell. 1984;6:721–741.
[20] Ching J, Chen YJ. Transitional Markov Chain Monte Carlo method for Bayesian model updating, model class selection, and model averaging. J. Eng. Mech. 2007;133:816–832.
[21] Muto M, Beck JL. Bayesian updating and model class selection for hysteretic structural models using Stochastic simulation. J. Vib. Control. 2008;14:7–34.
[22] Duane S, Kennedy AD, Pendleton BJ, et al. Hybrid Monte Carlo. Phys. Lett. B. 1987;195:216–222.
[23] Beskos A, Pillai N, Roberts G, et al. Optimal tuning of the hybrid Monte Carlo algorithm. Bernoulli. 2013;19:1501–1534.
[24] Hanson KM. Markov Chain Monte Carlo posterior sampling with the Hamiltonian Method. Proc. SPIE. 2001;4322:456–467.
[25] Ching J, Muto M, Beck JL. Structural model updating and health monitoring with incomplete modal data using Gibbs sampler. Comput. Aided Civ. Infrastruct. Eng. 2006;21:242–257.
[26] Izaguirre JA, Hampton SS. Shadow hybrid Monte Carlo: an efficient propagator in phase space of macromolecules. J. Comput. Phys. 2004;200:581–604.
[27] Boulkaibet I, Mthembu L, Marwala T, et al. Finite element model updating using the shadow hybrid Monte Carlo technique. Mech. Syst. Signal Process. 2015;52-53:115–132.
[28] Sweet CR, Hampton SS, Skeel RD, et al. A separable shadow Hamiltonian hybrid Monte Carlo method. J. Chem. Phys. 2009;131:174106. http://dx.doi.org/10.1063/1.3253687
[29] Boulkaibet I, Mthembu L, Marwala T, et al. Finite element model updating using the separable shadow hybrid Monte Carlo technique. IMAC XXXII; 2014 February 3–6; Orlando (FL).
[30] Goller B, Schuëller GI. Investigation of model uncertainties in Bayesian structural model updating. J. Sound Vib. 2011;330:6122–6136.
[31] Hanson KM. Markov Chain Monte Carlo posterior sampling with the Hamiltonian method. Proc. SPIE. 2001;4322:456–467.
[32] Skeel RD, Tupper PF. Mathematical issues in molecular dynamics. Banff International Research Station Reports. Alberta; 2005.
[33] Huang W, Leimkuhler B. The adaptive Verlet method. SIAM J. Sci. Comput. 1997;18:239–256.
[34] Blanes S, Casas F, Murua A. On the numerical integration of ordinary differential equations by processed methods. SIAM J. Numer. Anal. 2004;42:531–552.
[35] Neal RM. Suppressing random walks in Markov Chain Monte Carlo using ordered over relaxation. In Learning in graphical models. Netherlands: Springer; 1998. p. 205–228.
[36] Chen T, Fox EB, Guestrin C. Stochastic gradient Hamiltonian Monte Carlo. Proceedings of the 31 st International Conference on Machine Learning; Vol. 32; Beijing, China; 2014.
[37] Welling M, Teh YW. Bayesian learning via stochastic gradient Langevin dynamics. In: Proceedings of the 28th International Conference on Machine Learning (ICML-11); 2011; p. 681–688.

[38] Balmes E. Predicted variability and differences between tests of a single structure. In: Proceedings of the International Modal Analysis Conference IMAC XVI; 1998; Santa Barbara, CA; p. 558–564.
[39] Degener M, Hermes M. Ground vibration test and finite element analysis of the GARTEUR SM-AG19 tested. Deutsche Forschungsanstalt für Luft und Raumfahrt e. V. Institut für Aeroelastik, IB 232-96 J 08. 1996.
[40] Carvallo J, Datta BN, Gupta A, et al. A direct method for model updating with incomplete measured data and without spurious modes. Mech. Syst. Signal Process. 2007;21:2715–2731.
[41] Datta BN. Finite-element model updating, eigenstructure assignment and eigenvalue embedding techniques for vibrating systems. Mech. Syst. Signal Process. 2002;16:83–96.
[42] Guyon I, Elisseeff A. An introduction to variable and feature selection. J. Mach. Learn. Res. 2003;3:1157–1182.
[43] Link M, Friswell MI. Working group 1: generation of validated structural dynamic models – results of a benchmark study utilising the garteur sm-ag19 test-bed. Mech. Syst. Signal Process. 2003;17:9–20.